Ann Nucl Med (2007) 21:455–462
DOI 10.1007/s12149-007-0049-4

ORIGINAL ARTICLE

An atlas-based image registration method for dopamine receptor imaging with PET in rats

**Yojiro Sakiyama · Kentaro Hatano · Toshihisa Tajima
Takashi Kato · Yasuhiro Kawasumi · Mitsuru Suzuki
Kengo Ito**

Received: 8 February 2007 / Accepted: 11 June 2007

Abstract For analysis of in vivo dopamine receptor binding in the rat brain by positron emission tomography (PET), a convenient method to obtain precise anatomical registration for striatum and cerebellum on the PET image was developed. On the PET measurements, a control, an anesthetized rat was positioned in a stereotaxic holder so that the horizontal plane of the PET image would be parallel to the horizontal plane of the brain atlas. After the positioning, [^{11}C]raclopride was intravenously injected into the rats and scanned to obtain PET images of dopamine D_2 receptor in the brain. The striatum was bilaterally identified in the obtained PET image. The atlas-based regions of interest (ROIs) of the whole brain were preliminarily created according to the atlas, and were superimposed on an early phase PET image. The early phase PET image was compatible to the whole brain ROI in the atlas, which enabled determination of striatal and cerebellar ROI difficult to determine by the PET image alone. Using the cerebellar radioactivity as a reference input function, rate constants between the free/nonspecific compartment and the receptor bound compartment (k_3 and k_4) were calculated by a two-parameter compartment model, and the binding potential (k_3/k_4) was estimated. The binding potential and its coefficients of variation were 1.56 ± 0.30, 19.3% in Wistar rats, 1.05 ± 0.14, 13.4% in Sprague–Dawley (SD) rats, and 1.29 ± 0.07, 5.2% in Fischer F344 rats, in which binding potential in Wistar rats was significantly higher than that in SD rats. This method is objective and convenient in routine use for PET studies in rats, regardless of differences in the rat strains.

Keywords PET · Atlas · Raclopride · Receptor · Rat

Y. Sakiyama · K. Hatano (✉) · T. Tajima · T. Kato ·
Y. Kawasumi · M. Suzuki · K. Ito
Department of Brain Science and Molecular Imaging, National Institute for Longevity Sciences, 36-3 Gengo, Morioka-cho, Obu 474-8522, Japan
e-mail: hatanok@nils.go.jp

Introduction

Animal positron emission tomography (PET) studies are of great value because they can provide insights that are directly unavailable by human PET studies, such as validation of non-clinical drugs or invasive measurements under anesthesia. Although ex vivo autoradiography and/or tissue counting technique can in part serve such roles, these methods are laborious because they need many animals to obtain dynamic data, and are subject to interanimal variation. Thus, the need for PET studies that permit dynamic and repetitive measurements using a minimum number of animals has been recognized. Especially, PET imaging using rodents has been widely applied to investigate the in vivo dopaminergic neurotransmission pathway, including postsynaptic dopamine receptors [1–14], presynaptic dopamine transporters [13, 15, 16], and in vivo monitoring of dopamine receptor gene expression [17–19]. A functional magnetic resonance imaging (MRI) technique has also been used to investigate dopaminergic neuronal function using rats [20]. One of the reasons why many animal PET scientists have focused on the dopaminergic system is its possibility to detect striatal radioactivity by the use of a conventional animal PET scanner. In contrast to other neuronal systems, dopamine receptors are locally expressed in small striatal regions. In addition, because dopamine receptors are scarce in the cerebellum [21], the cerebellum can be used as a reference region to quantify dopa-

mine receptor function with no need for tedious blood sampling.

In most of these studies, the exact determination of regions of interest (ROIs) is difficult because of the coarse spatial resolution of a PET camera. In addition, PET image per se provides no anatomical information. Therefore, the determination of ROIs solely by PET image depends more or less on the subjectivity of scientists. A recent high-resolution PET imaging technique using small rodents—micro-PET—has a potential to solve this problem [2, 5, 7, 10, 16]; however, the image itself also provides no anatomical information. To overcome this problem, a 3D digital map developed at the University of California Los Angeles (UCLA) can assist anatomical interpretation in micro-PET studies [16]; however, the apparatus and software are not available in ordinary laboratories, and thus a convenient method for anatomical registration of the rat brain image with conventional animal PET scanner is expected.

Against this background, a convenient method for anatomical registration of the PET images of rats was investigated with the aid of the published atlas of the rat brain [22]. We accomplished anatomical matching between PET images and the atlas by adjusting the scanner axis to the horizontal plane determined on the atlas, and by superimposing the atlas-based whole brain ROIs on the PET images. This technique was extended to determine striatal and cerebellar ROIs enabling quantification of dopamine receptor function of the rat brain. In addition, because the atlas is published on the basis of a study of 130 adult male Wistar rats with a weight range of 270–310 g, we investigated whether this method is applicable to rats of various strains as well.

Methods

Materials

Desmethyl derivative R(+)-raclopride was purchased from commercial sources (Research Biochemicals International, Natick, MA, USA). [^{11}C]raclopride was prepared as described in the earlier report with a slight modification [23]. In brief, [^{11}C]CO_2 was produced by the proton irradiation of N_2 (20 μA, 40 min) by a small cyclotron (CYPRIS HM-18, Sumitomo Heavy Industries, Tokyo, Japan). [^{11}C]CH_3I obtained from [^{11}C]CO_2 following the usual procedure was trapped in 0.3 ml of dimethylsulfoxide containing 1 mg of desmethyl raclopride hydrochloride and 3 μl of 5N NaOH using the automated synthesis system (CUPID, Sumitomo Heavy Industries). The solution was heated at 60°C for 2 min and applied to preparative high performance liquid chromatography (HPLC). Capcellpack UG120 column (5 μm, φ20 × 250 mm, Shiseido, Tokyo, Japan) was used with 10 mM phosphate : acetonitrile (67 : 33, v/v) at a flow rate of 10 ml/min. The collected [^{11}C]raclopride fraction was evaporated to dryness and the residue was dissolved in physiological saline; 40 min after the end of irradiation, 663 ± 253 MBq (n = 18) of [^{11}C]raclopride was obtained. A small portion of the obtained product was analyzed with Capcellpack UG120 column (5 μm, ϕ4.6 × 150 mm, Shiseido) and 10 mM phosphate : acetonitrile (80 : 20, v/v) at a flow rate of 2 ml/min. The radiochemical purity exceeded 99%. The specific activity was 22.3 ± 17.3 GBq/μmol.

Animals

Wistar (10 weeks, 300–350 g; n = 4), Sprague–Dawley (SD; 10 weeks, 300–350 g, n = 4) and Fischer F344 (6 months, 350–400 g, n = 4) male rats were used for the present experiment. Wistar rats and SD rats were supplied by Shizuoka Laboratory Animals Center (Hamamatsu, Japan), and F344 rats were supplied by Charles River Labs (Yokohama, Japan). The rats were initially anesthetized with chloral hydrate (400 mg/kg i.p.). During the experiment the anesthetized rats were maintained with a continuous infusion of chloral hydrate (100 mg kg^{-1} h^{-1}, i.v.).

The present animal study was approved by the Animal Care and Use Committee of the National Institute for Longevity Sciences.

Positioning

Prior to the PET scanning, the anesthetized rat was fixed in a prone position with a holder, a modification of a stereotaxic holder for physiological experiments (Hamamatsu Photonics, Hamamatsu, Japan). The holder and its attachment including an incision bar and ear bar are all made of polyacrylate to eliminate artifacts during the scanning. For anatomical registration of the PET image, we used the atlas of Paxinos and Watson [22]. This atlas was prepared as a map for physiological experiments, representing 76 coronal cross sections of a rat brain with 0.2–0.5 mm intervals in photographs with free-hand drawings. The topography is based on a three-dimensional coordinate system, in which each cross section was vertical to the horizontal plane determined so that the distance of heights between the incision bar and the horizontal plane passing through the interaural line is 3.3 mm. On the measurement, the vertical interval (3.3 mm) was fixed in each rat in order to match the horizontal orientation between the scanner axis and the horizontal plane of the atlas. The head skin of the rat

was incised to expose bregma, which was positioned in the center of the field of view using a laser beam attached to the scanner. Of 76 coronal sections, 7 sections of 6.70 mm, 3.20 mm, 0.20 mm, anterior and 3.30 mm, 6.72 mm, 9.80 mm, 12.8 mm posterior from the bregma, which consistently corresponds to the PET images with 3.25 mm interval, were employed for the ROI analysis. In addition, a small amount of tracer (about 200 kBq/100 μl) was placed on the bregma to confirm that the coronal plane crossing the bregma corresponds to the coronal plane crossing the center of the striatum. A small cotton ball with a diameter of less than 2 mm in the dispenser tip was immersed with diluted solution of radioactivity as the location marker of bregma.

PET procedures

Each rat underwent one PET scanning acquired with [^{11}C]raclopride under the anesthetized, resting condition. The data acquisition protocol was followed by the same protocol as described earlier [24]. The SHR-2000 PET camera (Hamamatsu Photonics) was used and provided a 14-slice image set at 3.25-mm intervals with image spatial resolution of 3.5 mm full-width at half-maximum [25]. Correction of photon attenuation was carried out with transmission data obtained by rotating the ^{68}Ge/^{68}Ga rod source. Subsequently, 8–12 MBq of a [^{11}C]raclopride was injected into rats through a cannula inserted into tail vein and simultaneously scanning was started. Data were dynamically acquired 64 min (1 min × 64 frames), in which the first 60 min was used for the data analysis.

Data analysis

The tomographic images were reconstructed using a Butterworth filter with a cutoff frequency of 144 cycles/cm. To measure the regional radioactivity in the rat brain, atlas-based ROIs were superimposed to PET images acquired with [^{11}C]raclopride. First, whether the atlas-based ROIs accurately corresponded to the whole brain PET images was confirmed by superimposing the atlas-based ROIs to early phase PET images (average of 1–10 min). After the confirmation, the atlas-based ROIs were superimposed to the later phase PET images (average of 15–45 min) and the striatal and cerebellar ROIs were determined.

$$\%\mathrm{ID/ml} = \frac{\text{Tissue radioactivity (Bq/ml)}}{\text{Injected dose (Bq)}} \times 100$$

The tissue uptake of each tracer was evaluated as the percentage of injected dosage per volume tissue (%ID/ml) calculated by the following equation:

$$\%\mathrm{ID/ml} = \frac{\text{tissue radioactivity (Bq/ml)}}{\text{injected dosage (Bq)}} \times 100.$$

The most convenient techniques for quantitative in vivo dopamine receptor binding, at present, are based on a two-parameter compartment model using the cerebellum as an indirect input function [26, 27]. The kinetic parameters were calculated according to the model, which can be written with the following equation:

$$\frac{dC_b(t)}{dt} = k_3 C_{ce}(t) - k_4 C_b(t).$$

$$\frac{dC_b(t)}{dt} = k_3 \times C_{ce}(t) - k_4 C_b(t).$$

In the equation, C_b is the radioactivity of the receptor-bound compartment, C_{ce} the radioactivity of the free/nonspecific compartment (identical to the cerebellar radioactivity); k_3 is the rate constant from the free/nonspecific ligand to the receptor-bound ligand compartment, which is proportional to the bimolecular association rate (k_{on}) and the number of receptors (B_{max}); k_4 is the rate constant from the receptor-bound ligand compartment to the free/nonspecific ligand compartment, which is equivalent to the dissociation rate from the receptors (k_{off}). The ratio k_3/k_4 is the binding potential equivalent to B_{max}/K_d, in which K_d is the dissociation constant equivalent to the ratio of the molecular dissociation rate to the association rate [28]. The cerebellar uptake was used for the reference of the free/nonspecific compartment, and the difference between the striatal uptake and cerebellar uptake was used for the receptor-bound compartment. The optimal values of k_3 and k_4 were obtained by using a nonlinear least-squares method, and the binding potential (k_3/k_4) was calculated. In addition, to evaluate the accuracy of the kinetic parameters obtained by the present method in each strain of rats, the coefficient of variation (CV) of the binding potential was calculated by the percentage of the ratio of the standard deviation (SD) to the mean value of each strain of rats. All analysis procedures were performed on a workstation with an image analysis software Dr. View version 4.0 (Asahi Kasei Joho System, Tokyo, Japan).

Tissue slice preparation

To validate the above image registration technique and to determine structural differences between the three kinds of rat strain, tissue slice samples were obtained from each rat brain after the PET experiments. The brains were dissected, and treated in diluted (10%) formaldehyde solution for 1 week, followed by hemoglobin

(HB) staining to obtain slices that cross striatal and cerebellar regions.

Results

The position of the head of a Wistar rat, drawings of the rat brain in the atlas, and the PET images of [^{11}C]raclopride are schematically shown in Fig. 1. As shown in Fig. 1c, tracer spot on the bregma as a fiducial marker could be observed definitely in the coronal PET image acquired in the early phase (average of 1–10 min). In the same coronal plane crossing the bregma, two hot spots, striatal images, were also identified definitely in the later phase PET image (average of 15–45 min).

Figure 2 shows a result of the procedure to determine ROIs representing in a descending order. The early phase PET images (Fig. 2b) did not give any precise structural information by themselves; however, the contour of the brain discernible in the early phase PET

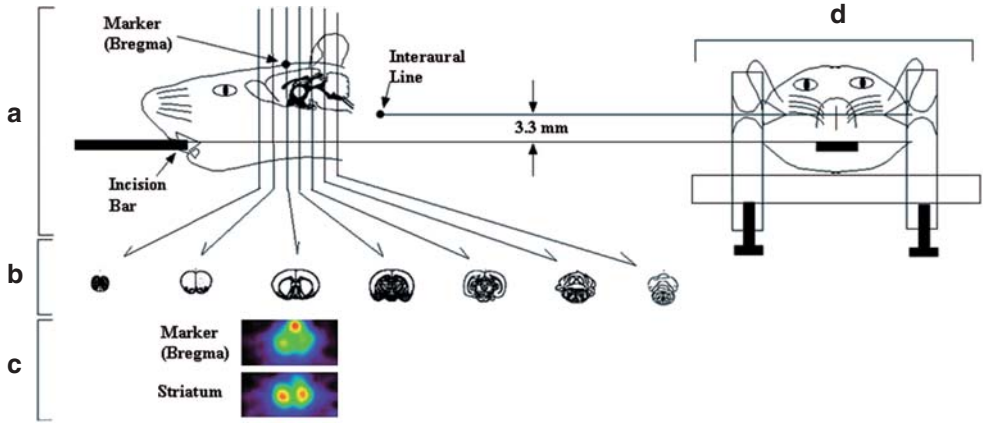

Fig. 1 **a** Schematic representation of the head of a Wistar rat fixed on a stereotaxic holder in which deviation of heights between incision bar and interaural line should be 3.3 mm to match the horizontal plane of the atlas. **b** Drawings of atlas sections. The distance of each drawing from the bregma is +6.70 mm, +3.20 mm, +0.20 mm, –3.30 mm, –6.72 mm, –9.80 mm, and –12.8 mm. The interval approximately corresponds to the slice interval of positron emission tomography (PET) images. **c** A coronal plane of PET image crossing the bregma (*upper*, early phase image of [^{11}C] raclopride) corresponding to a coronal plane crossing the center of the striatum (*lower*, later phase image). **d** A coronal scheme of the hand-made ear bar made of polyacrylate. The ear bar was preliminarily fixed on the rat head so as to correspond to the position of the interaural line, followed by the attachment on the stereotaxic bed parallel to the scanner axis

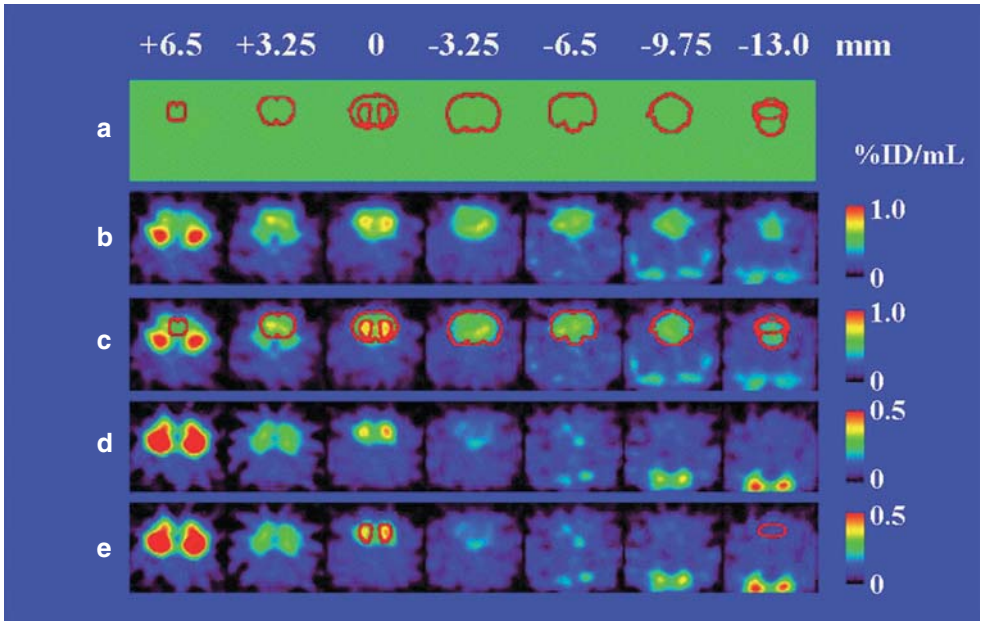

Fig. 2 Atlas-based regions of interest (ROIs) determined in a descending order. *Upper numerical* denotes distance from bregma (mm). **a** Free-hand drawings of the edge of the whole-brain region extracted from the atlas sections shown in Fig. 1b. **b** Early phase images (1–10 min) of a brain of Wistar rat. **c** Early phase images with (**a**) superimposed. **d** Later phase images (15–45 min). **e** Later phase images with drawings of striatum and cerebellum superimposed

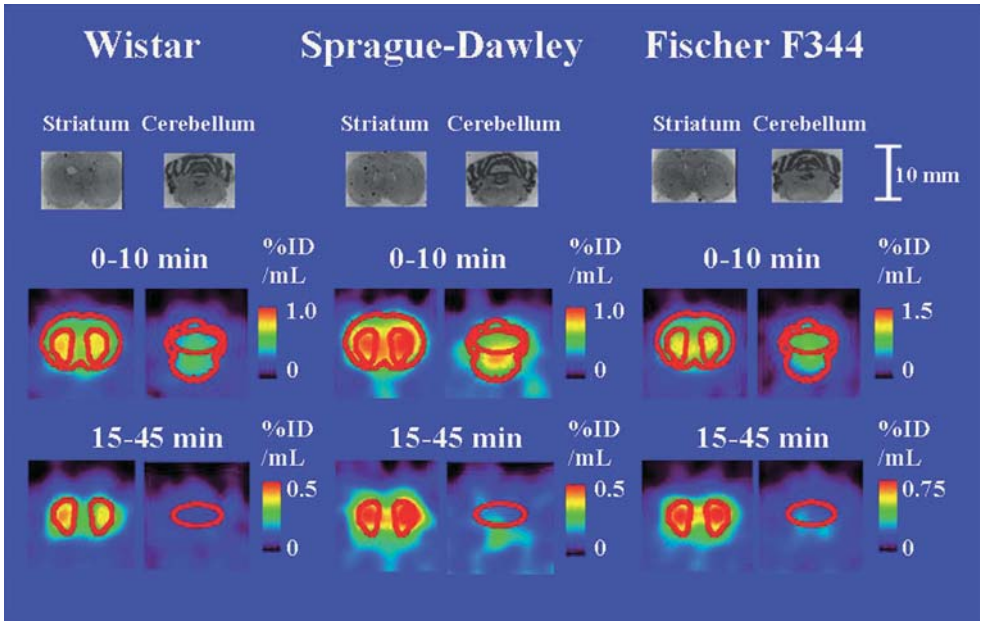

Fig. 3 Atlas-based determination of ROIs in the PET images of rats of various strains. *Upper row* shows stained brain tissue slices of rats of three different strains. These slices were sectioned by coronal planes passing the center of the striatum and the cerebellum. *Lower two rows* were PET images of rat brain acquired with [^{11}C]raclopride, anatomically corresponding to the upper tissue slices. Values were expressed as % ID/ml

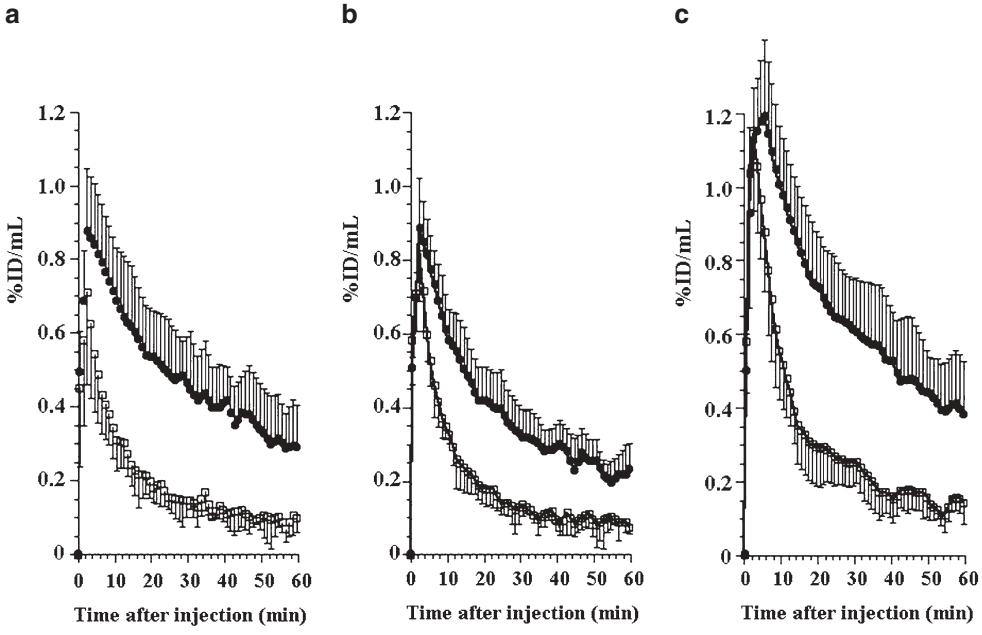

Fig. 4 Time–activity curves of striatum (*filled circle*) and cerebellum (*open square*) following intravenous injection of [^{11}C]raclopride in rats of various strains. **(a)** Wistar rat; **(b)** Sprague–Dawley rat; **(c)** Fischer F344 rat. Values were expressed as the percentage of the injected dosage per milliliter tissue (%ID/ml). Data are mean ± standard deviation of four rats of each strain

images was largely compatible with the whole-brain ROIs (Fig. 2c). Next, the striatal and the cerebellar ROIs included in the whole-brain ROIs were superimposed on the later phase PET images (Fig. 2d, e). The bilateral hot areas observed in the PET image corresponded well to the striatal ROIs. The cerebellar ROI, although no hot spots were observed in the later phase cerebellar image because of the scarce of dopamine receptor, could be determined using this procedure.

The tissue slice samples and the corresponding PET images in both striatal and cerebellar regions obtained from rats of the three strains, Wistar, SD, and Fischer F344, are shown in Fig. 3. As shown obviously, no species differences in the contour of tissue slices were observed in either region. In addition, the contour of tissue slices was shown to largely correspond to the contour of the early phase PET images.

Figure 4 shows the time–activity curves of the striatum and the cerebellum following intravenous injection of [^{11}C]raclopride into the rats of each strain. To obtain these curves the same atlas-based ROIs were used on the basis of the result of Fig. 3. Both the striatal and

Table 1 Rate constants and the binding potential of [^{11}C]raclopride obtained by atlas-based region of interest analysis in the rats of various strains

	Mean	SD	CV
k_3 (1/min)			
Wistar	0.109	0.021	19.7
Sprague–Dawley	0.066	0.013	19.4
F344	0.073	0.031	42.2
k_4 (1/min)			
Wistar	0.071	0.021	29.4
Sprague–Dawley	0.062	0.008	12.3
F344	0.056	0.023	40.9
BP			
Wistar	1.56	0.30	19.3
Sprague–Dawley	1.05	0.14	13.4
F344	1.29	0.07	5.2

CV coefficient of variation, *BP* binding potential

cerebellar uptake reached a peak 2–3 min after tracer injection, and the subsequent decrease of the cerebellar uptake was higher than the striatal uptake. The specific binding, estimated by the striatal minus the cerebellar uptake, reached a plateau approximately 20 min after tracer injection. Although absolute values of the tissue uptake were quite different, the patterns were almost the same among strains. The results of the kinetic analyses were summarized in Table 1. The binding potential and its coefficients of variation were 1.56 ± 0.30, 19.3% in Wistar rats, 1.05 ± 0.14, 13.4% in SD rats and 1.29 ± 0.07, 5.2% in Fischer F344 rats. A statistically significant difference was found in the binding potential between Wistar rats and SD rats [$P < 0.01$, by one-way analysis of variance with Fisher's protected least significant difference (PLSD)].

Discussion

In the PET study using rats, a method of anatomical interpretation of PET images is a prerequisite for the exact determination of ROIs to use for the following analysis procedures. As described before, in most of the PET studies in rats reported, PET images were anatomically interpreted mostly by visual inspection, and thus determination of ROIs by PET image depends more or less on the subjectivity of scientists. One approach to cope with this problem is to accomplish anatomical registration with MRI images [9, 29–31]. This approach is more prominent than visual inspection because of its direct way of anatomical registration. However, this method requires skilled technique in superimposing PET images to MRI images, in addition to the fact that MRI for animals is not available in most ordinary laboratories. Another approach is to use 3D rat brain atlas-derived volumes of interest. This method is outstanding in that accurate and unbiased registration can be accomplished with no use of computed tomography or MRI, although this method is specifically developed for micro-PET studies and requires dedicated software for automated registration [16]. The method described here is a more convenient and objective approach by utilizing the relationship between PET images and anatomical markers on the body surface. We have confirmed as shown in Fig. 1 that the two hot spots seen in the later phase PET image were certain to be the striatal PET images because they were seen in the same coronal plane crossing the bregma on which a radioactive marker was applied. It has also been demonstrated that the contour of the early phase PET images was compatible to the whole-brain contour of the seven slice sections in the atlas, and the hot spot of radioactivity seen in the late phase image also exactly matched the region of striatum in the atlas section. Therefore, atlas-based precise anatomical registration can be accomplished only if care is taken in the positioning of the rat head. In addition, it is generally difficult to define the cerebellar ROI by PET image alone because of the scarcity of dopamine receptors; however, the geometrical compatibility between PET image and atlas enabled definition of cerebellar ROI as shown in Fig. 2. The obtained cerebellar time–activity curve can be used as an input function, which is convenient for the kinetic analysis rather than the use of the plasma input function.

This method is applicable on the assumption that the spatial relationship between bregma on the skull and various brain regions in the intracranial space remains constant. The result of tissue slice studies from various rat strains as shown Fig. 3 suggested that even though the structural difference between rat strains was relatively small, interanimal differences in the same species would be much smaller. Interestingly, Fig. 3 also suggested that the anatomy of a 6-month-old F344 rat was similar in size and shape to other normal adult rats. Anatomical studies using albino rats have reported a high correlation between the position of skull points and cerebral structures [32]. It has also been demonstrated that the bone length of the skull of senescent Fischer male rats was approximately 5% larger than that of 6-month old rats [33]. In other words, if the distance between the bregma and the center of the cerebellum is approximately 13 mm, the distance between the bregma and the center of the cerebellum will not exceed 14 mm in the senescent male rat (within the range feasible to measure both regions). This evidence together with the present tissue studies suggests that the structure of the rat brain in general does not differ appreciably among animals, strains, and ages. It is also obvious in Fig. 3

that the atlas-based ROIs can commonly be applicable to PET images of all rat strains. This is valuable in a practical way because SD rats as well as Wistar rats are widely used in neuroscience research, and the Fischer F344 rat has also been used frequently in aging research. So far as striatal dopamine receptor imaging is concerned, this method seems to be adequate for anatomical registration using any strains of rats with a low-resolution PET scanner.

Our results also showed higher D_2 receptor binding potential in Wistar rats than in SD rats, as shown in Table 1. As shown in Fig. 4, the difference in the binding potential between these strains could be owing to the difference in specific binding (striatal minus cerebellar radioactivity) between the strains. This finding is in part supported by autographic studies demonstrating that Wistar rats exhibited higher D_2 receptor levels than SD rats in the dorsolateral part of the caudate-putamen [34]. On the other hand, higher binding potential in adult Wistar rats than in senescent F344 rats was observed. This observation is unlikely to reflect the strain differences because age-related reduction in D_2-receptor binding in F344 rats has been reported [8]. Additional experiments using adult F344 rats will be necessary to elucidate the cause of this difference between these strains.

This method is convenient for routine use and is applicable to various rat models, such as the 6-OHDA-lesioned rat model [1], conscious rat model [3], Huntington's disease model [6, 10], genetically modified rodent models [7, 17, 19], aging rat model [8], and binge cocaine administration model [11]. The combined use of PET with microdialysis also provides valuable information regarding dopaminergic neurotransmission [2, 20]. These studies have possibilities for providing insight for the investigation of neurodegenerative disorders or mechanism of drug abuse. This technique will also serve as a bridge between human and rodent studies, because it is capable of comparing the same functional parameters that are imaged with PET in humans.

Conclusions

A stereotaxic method of atlas-based image registration of the rat brain was developed for dopamine D_2 receptor mapping by means of [^{11}C]raclopride and PET. This method provides PET scientists with a convenient, efficient, and objective method of analysis, which is an alternative to the tedious, manual ROIs methods. This method is applicable to various species of rat for various pharmacological and physiological studies.

Acknowledgments The authors thank Dr. H. Toyama, the National Institute of Radiological Sciences, for her technical support in the data analysis of animal PET study. This research was supported by Health Sciences Research Grants for Comprehensive Research on Aging and Health and for Research on Brain Science from the Ministry of Health, Labour and Welfare, Japan.

References

1. Inaji M, Okauchi T, Ando K, Maeda J, Nagai Y, Yoshizaki T, et al. Correlation between quantitative imaging and behavior in unilaterally 6-OHDA-lesioned rats. Brain Res 2005; 1064:136–45.
2. Schiffer WK, Alexoff DL, Shea C, Logan J, Dewey SL. Development of a simultaneous PET/microdialysis method to identify the optimal dose of 11C-raclopride for small animal imaging. J Neurosci Methods 2005;144:25–34.
3. Momosaki S, Hatano K, Kawasumi Y, Kato T, Hosoi R, Kobayashi K, et al. Rat-PET study without anesthesia: anesthetics modify the dopamine D1 receptor binding in rat brain. Synapse 2004;54:207–13.
4. Houston GC, Hume SP, Hirani E, Goggi JL, Grasby PM. Temporal characterisation of amphetamine-induced dopamine release assessed with [11C]raclopride in anaesthetized rodents. Synapse 2004;51:206–12.
5. Alexoff DL, Vaska P, Marsteller D, Gerasimov T, Li J, Logan J, et al. Reproducibility of 11C-raclopride binding in the rat brain measured with the microPET R4: effects of scatter correction and tracer specific activity. J Nucl Med 2003;44: 815–22.
6. Ishiwata K, Ogi N, Hayakawa N, Umegaki H, Nagaoka T, Oda K, et al. Positron emission tomography and ex vivo and in vitro autoradiography studies on dopamine D2-like receptor degeneration in the quinolinic acid-lesioned rat striatum: comparison of [11C]raclopride, [11C]nemonapride and [11C]N-methylspiperone. Nucl Med Biol 2002;29:307–16.
7. Thanos PK, Taintor NB, Alexoff D, Vaska P, Logan J, Grandy DK, et al. In vivo comparative imaging of dopamine D2 knockout and wild-type mice with (11)C-raclopride and microPET. J Nucl Med 2002;43:1570–7.
8. Suzuki M, Hatano K, Sakiyama Y, Kawasumi Y, Kato T, Ito K. Age-related changes of dopamine D1-like and D2-like receptor binding in the F344/N rat striatum revealed by positron emission tomography and in vitro receptor autoradiography. Synapse 2001;41:285–93.
9. Hayakawa N, Uemura K, Ishiwata K, Shimada Y, Ogi N, Nagaoka T, et al. A PET-MRI registration technique for PET studies of the rat brain. Nucl Med Biol 2000;27:121–5.
10. Araujo DM, Cherry SR, Tatsukawa KJ, Toyokuni T, Kornblum HI. Deficits in striatal dopamine D(2) receptors and energy metabolism detected by in vivo microPET imaging in a rat model of Huntington's disease. Exp Neurol 2000;166:287–97.
11. Tsukada H, Kreuter J, Maggos CE, Unterwald EM, Kakiuchi T, Nishiyama S, et al. Effects of binge pattern cocaine administration on dopamine D1 and D2 receptors in the rat brain: an in vivo study using positron emission tomography. J Neurosci 1996;16:7670–7.
12. Hume SP, Opacka-Juffry J, Myers R, Ahier RG, Ashworth S, Brooks DJ, et al. Effect of L-dopa and 6-hydroxydopamine lesioning on [11C]raclopride binding in rat striatum, quantified using PET. Synapse 1995;21:45–53.
13. Hume SP, Myers R, Bloomfield PM, Opacka-Juffry J, Cremer JE, Ahier RG, et al. Quantitation of carbon-11-labeled

raclopride in rat striatum using positron emission tomography. Synapse 1992;12:47–54.
14. Tajima T, Hatano K, Suzuki M, Ogawa M, Sakiyama Y, Kato T, et al. Increased binding potential of [11C]raclopride during unilateral continuous microinjection of nicotine in rat striatum by positron emission tomography. Synapse (in press).
15. Hume SP, Lammertsma AA, Myers R, Rajeswaran S, Bloomfield PM, Ashworth S, et al. The potential of high-resolution positron emission tomography to monitor striatal dopaminergic function in rat models of disease. J Neurosci Methods 1996;67:103–12.
16. Rubins DJ, Melega WP, Lacan G, Way B, Plenevaux A, Luxen A, et al. Development and evaluation of an automated atlas-based image analysis method for microPET studies of the rat brain. Neuroimage 2003;20:2100–18.
17. Ogawa O, Umegaki H, Ishiwata K, Asai Y, Ikari H, Oda K, et al. In vivo imaging of adenovirus-mediated over-expression of dopamine D2 receptors in rat striatum by positron emission tomography. Neuroreport 2000;11:743–8.
18. Aung W, Okauchi T, Sato M, Saito T, Nakagawa H, Ishihara H, et al. In-vivo PET imaging of inducible D2R reporter transgene expression using [11C]FLB 457 as reporter probe in living rats. Nucl Med Commun 2005;26:259–68.
19. Umegaki H, Ishiwata K, Ogawa O, Ingram DK, Roth GS, Yoshimura J, et al. In vivo assessment of adenoviral vector-mediated gene expression of dopamine D(2) receptors in the rat striatum by positron emission tomography. Synapse 2002;43:195–200.
20. Chen YC, Galpern WR, Brownell AL, Matthews RT, Bogdanov M, Isacson O, et al. Detection of dopaminergic neurotransmitter activity using pharmacologic MRI: correlation with PET, microdialysis, and behavioral data. Magn Reson Med 1997;38:389–98.
21. Seeman P. Brain dopamine receptors. Pharmacol Rev 1980; 32:229–313.
22. Paxinos G, Watson C. The rat brain in stereotaxic coordinates. 2nd ed. London: Academic; 1986.
23. Ehrin E, Gawell L, Högberg T, Paulis T, Ström P. Synthesis of [methoxy-^{3}H]- and [methoxy-^{11}C]-labelled raclopride: specific dopamine-D_2 receptor ligand. J Labelled Compds Radiopharm 1987;24:931–40.
24. Sakiyama Y, Ishiwata K, Ishii K, Oda K, Toyama H, Ishii S, et al. Evaluation of the brain uptake properties of [1-11C]labeled hexanoate in anesthetized cats by means of positron emission tomography. Ann Nucl Med 1996;10: 361–6.
25. Watanabe M, Uchida H, Okada K, Shimizu K, Satoh E, Yoshikawa T, et al. A high resolution PET for animal studies. IEEE Trans Med Imag 1992;11:577–80.
26. Eckernâs SA, Aquilonius SM, Hartvig P, Hagglünd J, Lundqvist H, Nagren K, et al. Positron emission tomography (PET) in the study of dopamine receptors in the primate brain: evaluation of a kinetic model using 11C-N-methyl-spiperone. Acta Neurol Scand 1987;75:168–78.
27. Lundberg T, Lindstrom LH, Hartvig P, Eckernâs SA, Ekblom B, Lundqvist H, et al. Striatal and frontal cortex binding of 11-C-labelled clozapine visualized by positron emission tomography (PET) in drug-free schizophrenics and healthy volunteers. Psychopharmacology (Berl) 1989;99:8–12.
28. Mintun MA, Raichle ME, Kilbourn MR, Wooten GF, Welch MJ. A quantitative model for the in vivo assessment of drug binding sites with positron emission tomography. Ann Neurol 1984;15:217–27.
29. Magata Y, Saji H, Choi SR, Tajima K, Takagaki T, Sasayama S, et al. Noninvasive measurement of cerebral blood flow and glucose metabolic rate in the rat with high-resolution animal positron emission tomography (PET): a novel in vivo approach for assessing drug action in the brains of small animals. Biol Pharm Bull 1995;18:753–6.
30. Ouchi Y, Tsukada H, Kakiuchi T, Nishiyama S, Futatsubashi M. Changes in cerebral blood flow and postsynaptic muscarinic cholinergic activity in rats with bilateral carotid artery ligation. J Nucl Med 1998;39:198–202.
31. Temma T, Magata Y, Kuge Y, Shimonaka S, Sano K, Katada Y, et al. Estimation of oxygen metabolism in a rat model of permanent ischemia using positron emission tomography with injectable15O-O2. J Cereb Blood Flow Metab 2006;26: 1577–83.
32. Slotnick BM, Brown DL. Variability in the stereotaxic position of cerebral points in the albino rat. Brain Res Bull 1980;5:135–9.
33. Riesenfeld A. Age changes on bone size and mass in two strains of senescent rats. Acta Anat (Basel) 1981;109:64–9.
34. Zamudio S, Fregoso T, Miranda A, De La Cruz F, Flores G. Strain differences of dopamine receptor levels and dopamine related behaviors in rats. Brain Res Bull 2005;65:339–47.